Chapter 1

Gentle introduction to the Thesis

1.1 Useful tools

The study of *Determination of the Mass Distribution in the Galactic Centre from the Stellar Motions* is impossible to perform without numerical simulations. For this purpose we use the fifth-order Runge-Kutta integrator with adaptive step-size control which is sufficiently precise.

1.2 Apocentre shift under spherical perturbation to the central potential

The first experiment we acquitted of was study of the apocentre shift of a test particle moving in the central potential field caused by the supermassive black hole (SMBH, $M_\bullet = 3.5 \times 10^6\ M_\odot$) in the Galactic Centre and influenced by a spherical perturbing potential.

The studied spherical perturbation has the power-law mass-density distribution $\rho_{\mathrm{per,\,S}}(r)$ with power-law index α and characteristic radius r_0:

$$\rho_{\mathrm{per,\,S}}(r) = \rho_0 \left(\frac{r}{r_0}\right)^{-\alpha} \tag{1.1}$$

From a given mass-density distribution $\rho_{\mathrm{per,\,S}}(r)$ one can compute the perturbing potential $\Phi_{\mathrm{per,\,S}}$ and mass distribution $M_{\mathrm{per,\,S}}$ of such spherical

perturbation

$$M_{\rm per,\,S} = kM_\bullet \left(\frac{r}{r_0}\right)^s, \tag{1.2}$$

$$\Phi_{\rm per,\,S} = \frac{kGM_\bullet}{(s-1)r_0}\left(\frac{r}{r_0}\right)^{s-1}, \tag{1.3}$$

where $s = 3-\alpha$ is the modified power-law index. We can define the apocentre shift of a test particle with unperturbed semi-major axis a and eccentricity e in the central potential perturbed by a spherical power-law in mass-density distribution $\delta\omega$ as follows:

$$\delta\omega = \frac{2k}{s-1}\left(\frac{a}{r_0}\right)^s \frac{\varepsilon}{e}\left[(2s+1)e\varepsilon^{2s-1}\mathcal{A} + (s+1)\varepsilon^{2s+1}\mathcal{B}\right], \tag{1.4}$$

where

$$\varepsilon = \sqrt{1-e^2}, \tag{1.5}$$

$$\mathcal{A} \equiv \int_0^\pi \frac{\mathrm{d}\varphi}{(1+e\cos\varphi)^{s+1}}, \tag{1.6}$$

$$\mathcal{B} \equiv \int_0^\pi \frac{\cos\phi\,\mathrm{d}\varphi}{(1+e\cos\varphi)^{s+2}}. \tag{1.7}$$

One can study how the $\delta\omega$ changes with the modified power-law index s:

$$\begin{aligned}\frac{\mathrm{d}\delta\omega}{\mathrm{d}s} = {} & \frac{2k\varepsilon^{2s}}{(s-1)e}\left(\frac{a}{r_0}\right)^s \times \\ & \times\left\{\left[\frac{1}{s-1}+\ln\left(\frac{a}{r_0}\right)+\ln(\varepsilon^2)\right]\left[(2s+1)e\mathcal{A}+(s+1)\varepsilon^2\mathcal{B}\right]\right. \\ & \left. + e\left[2\mathcal{A}+(2s+1)\mathcal{C}\right]+\varepsilon^2\left[\mathcal{B}+(s+1)\mathcal{D}\right]\right\},\end{aligned} \tag{1.8}$$

$$\begin{aligned}\frac{\mathrm{d}\ln(\delta\omega)}{\mathrm{d}s} = {} & \frac{e\left[2\mathcal{A}+(2s+1)\mathcal{C}\right]+\varepsilon^2\left[\mathcal{B}+(2s+1)\mathcal{D}\right]}{(2s+1)e\mathcal{A}+(s+1)\varepsilon^2\mathcal{B}} - \\ & -\left[\frac{1}{s-1}-\ln\left(\frac{a}{r_0}\right)-\ln(\varepsilon^2)\right],\end{aligned} \tag{1.9}$$

where

$$\mathcal{C} \equiv -\int_0^\pi \frac{\ln(1+e\cos\varphi)\,\mathrm{d}\varphi}{(1+e\cos\varphi)^{s+1}}, \tag{1.10}$$

$$\mathcal{D} \equiv -\int_0^\pi \frac{\cos\phi\ln(1+e\cos\varphi)\,\mathrm{d}\varphi}{(1+e\cos\varphi)^{s+2}}. \tag{1.11}$$

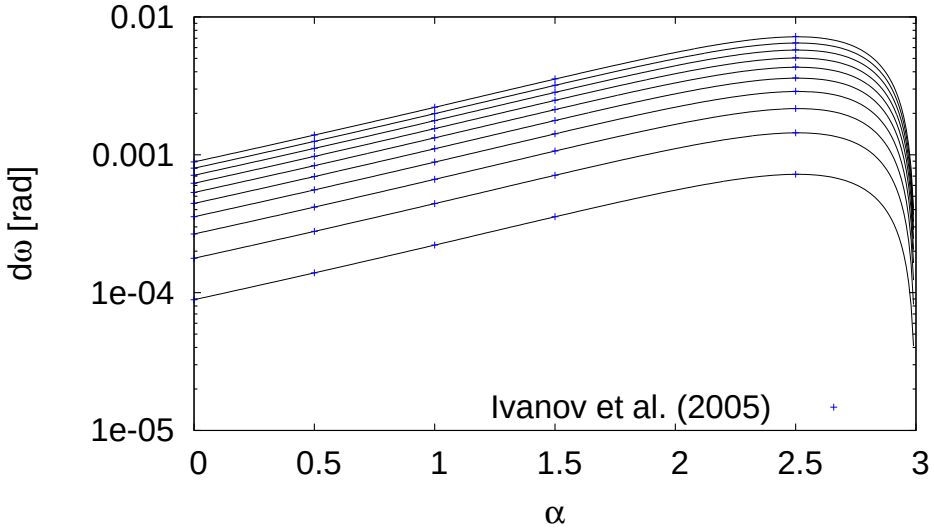

Figure 1.1: Apocentre shift of a test particle in the central potential perturbed by a spherical power-law in mass-density distribution with different power-law index α. Note the logarithmic scale of $\delta\omega$. The numerical results are in black, the blue crosses depict analytical values following Ivanov et al. (2005). The black curves differ in total perturbation mass $M_{\rm per} = kM_\bullet$ with equidistant steps $\Delta k = 10^{-3}$ and k values $k \in [10^{-3}, 10^{-2}]$, ordered from the lightest to the heaviest perturbation sequence from the bottom to the top.

We tested such analytical model with numerical simulation. We show the numerical result compared with several analytical points given in Ivanov et al. (2005) on the Fig. 1.1 . You can see the points obtained by analytical analysis in Ivanov et al. (2005) are consistent with the numerical model, therefore we can use numerical simulation with sufficient accuracy for estimate $\delta\omega$ for spherical perturbations, where we don't know the exact value from analytical formula (1.4).

1.3 Axi-symmetric perturbation

There are several axi-symmetric structures observed in the central parsec of our Galaxy. In our simulations we study effect of Kozai oscillations on orbital elements of a testing particle influenced by the central potential

perturbed by axi-symmetrical ring with potential $\Phi_{\rm R}(r)$

$$\Phi_{\rm per,\,R} = -2G\lambda\sqrt{\frac{a}{R}}k\mathcal{K}(k), \tag{1.12}$$

where

$$k^2 = \frac{4a_{\rm R}R}{(a_{\rm R}+R)^2+(z-z_{\rm R})^2}. \tag{1.13}$$

The equations of motion given by the problem Hamiltonian

$$H = 0.5(v_x^2+v_y^2+v_z^2) - \frac{1}{r} + \Phi_{\rm per,\,R} \tag{1.14}$$

then read

$$\begin{aligned}
\dot{x} &= v_x, && (1.15)\\
\dot{y} &= v_y, && (1.16)\\
\dot{z} &= v_z, && (1.17)\\
\dot{v}_x &= -\frac{x}{r^3} - G\lambda\sqrt{a_{\rm R}}kR^{-5/2}\mathcal{K}(k)x + 2\frac{G\lambda\sqrt{a_{\rm R}}}{\sqrt{R}(1-k^2)}{\rm C_A}\mathcal{E}(k)x, && (1.18)\\
\dot{v}_y &= -\frac{y}{r^3} - G\lambda\sqrt{a_{\rm R}}kR^{-5/2}\mathcal{K}(k)y + 2\frac{G\lambda\sqrt{a_{\rm R}}}{\sqrt{R}(1-k^2)}{\rm C_A}\mathcal{E}(k)y, && (1.19)\\
\dot{v}_z &= -\frac{z}{r^3} - \frac{G\lambda(z-z_{\rm R})k^3}{2\sqrt{a_{\rm R}}(1-k^2)}R^{-3/2}\mathcal{E}(k), && (1.20)
\end{aligned}$$

where

$${\rm C_A} = \frac{k}{2R^2}\left(1 - \frac{a_{\rm R}+R}{2a_{\rm R}}k^2\right). \tag{1.21}$$

In the system consisting of the central SMBH, axi-symmetrical perturbation and test particle we can study how much the averaged perturbing potential value changes with different initial eccentricity e_0 and initial argument of periapsis ω_0. From such experiment we obtain four distinct topologies of iso-contours of averaged perturbing potential with different values of constant c proportional to the $z-$component of the angular momentum $L_{\rm z}$

$$c = \sqrt{1-e^2}\cos i. \tag{1.22}$$

The four panels on Fig. 1.2 depicting c=0.0, c=0.2, c=0.4 and c=0.8. The higher value of c the lower maximal eccentricity $e_{\rm MAX}$ of possible trajectories given by (1.22).

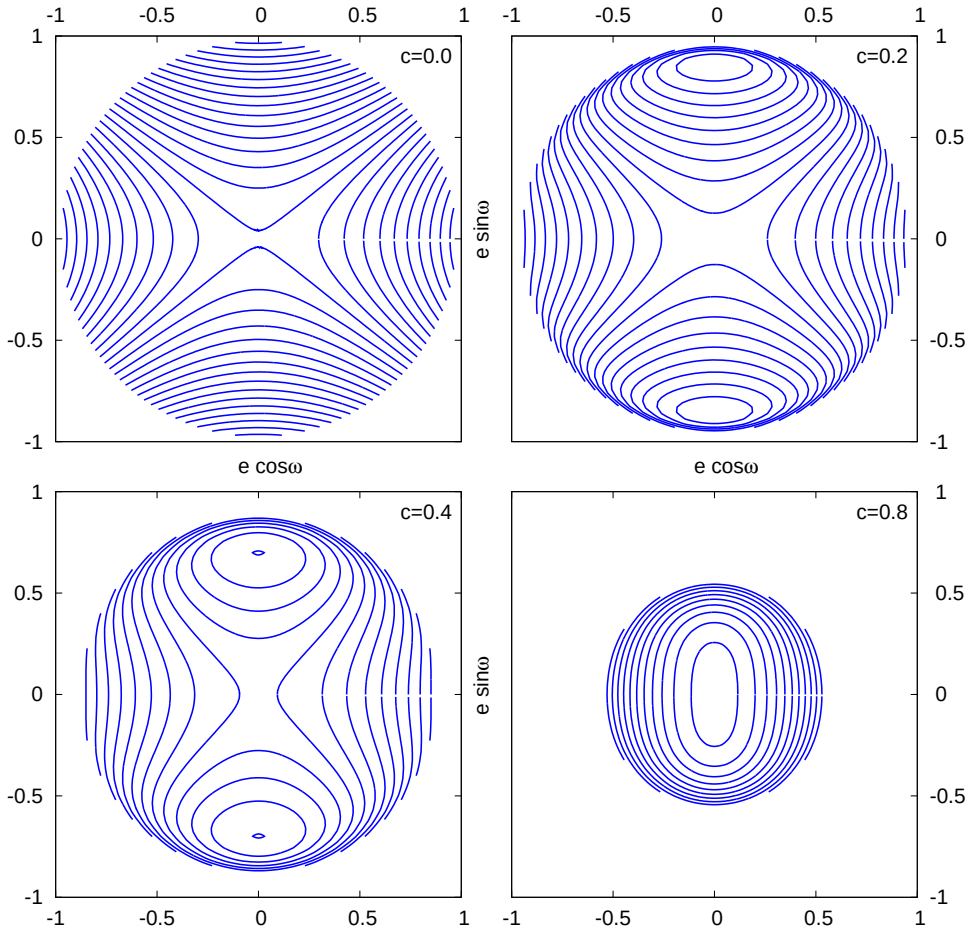

Figure 1.2: The four panels show iso-contours of averaged perturbing potential given by the axi-symmetric system (ring) with parameters $a_{\rm RING} = 10\,a$, $M_{\rm RING}= 5 \times 10^{-3}\,M_\bullet$, where $a = 13578.588 R_{\rm g}$ is the semi-major axis of the test particle (S2 star).

The value of the averaged perturbing potential is a quasi-constant of motion. Therefore, one can study time evolution of averaged orbital elements, namely of the averaged eccentricity $\langle e \rangle$ and the averaged argument of periapsis $\langle \omega \rangle$ with such figures (see Fig. 1.2), because the $\langle e \rangle$ and $\langle \omega \rangle$ should evolve around a specific iso-contour of $\langle \Phi_{\text{per, R}} \rangle$. On Fig. 1.3 we can see the time evolution of $\langle e \rangle$ and $\langle \omega \rangle$ projected onto a iso-contours diagram and time evolution of three averaged orbital elements of such trajectory, namely $\langle e \rangle(t)$, $\langle \omega \rangle(t)$, $\langle i \rangle(t)$.

1.4 Kozai oscillations in the Galactic Centre

The Kozai period is the time-scale on which the averaged orbital elements suffer significant changes in their values. We can study several configurations of sources of perturbation to the central SMBH potential in order to compare the values of Kozai periods as function of a, c, e_0, ω_0 and the composition of the perturbation taken into account. The Fig. **??** shows such dependence for one specific system setup.

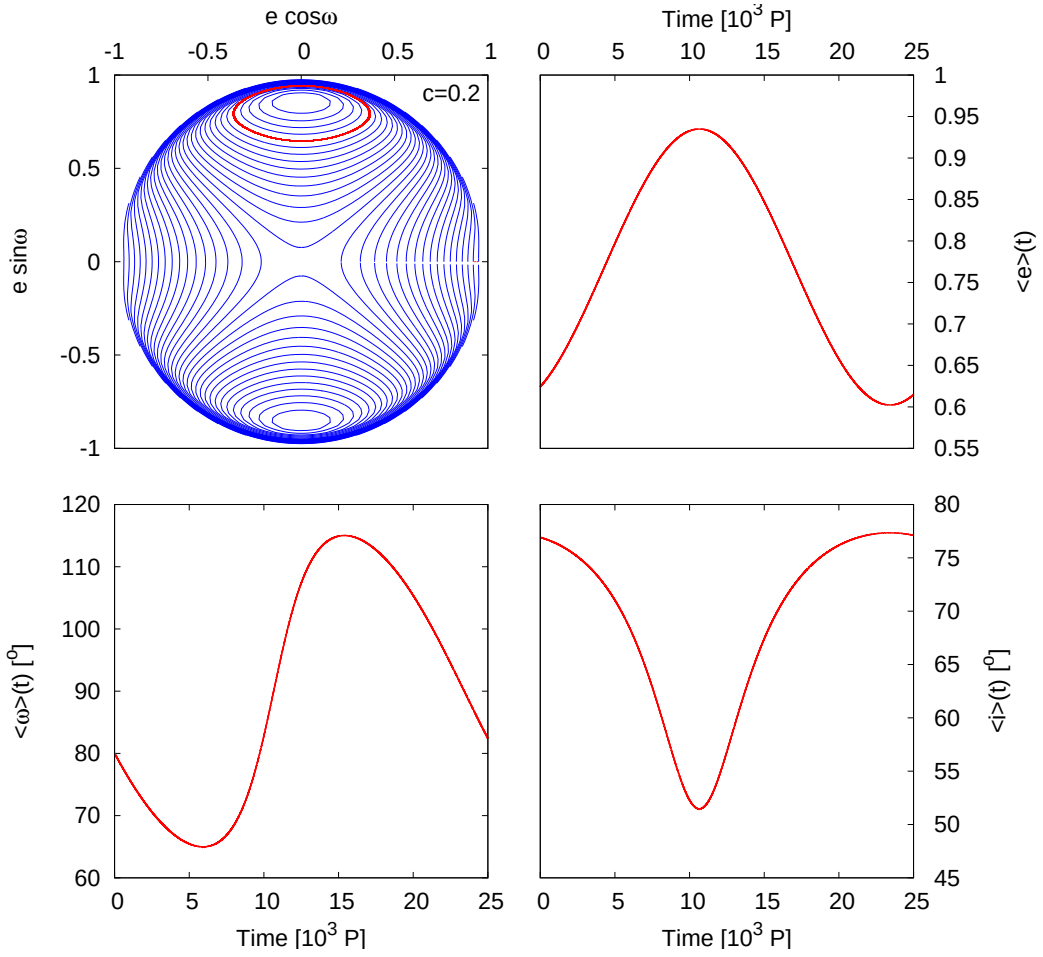

Figure 1.3: Time evolution of averaged orbital elements of a trajectory with $e_0 = 0.666$ and $\omega_0 = 80°$. Note that the red "trajectory" follows the iso-contour of $\langle \Phi_{\text{per, R}} \rangle \doteq -7.33 \times 10^{-8}$. On three remaining panels you can see the time evolution of averaged orbital elements eccentricity $\langle e \rangle(t)$, argument of periapsis $\langle \omega \rangle(t)$ and inclination $\langle i \rangle(t)$ over one Kozai period. Shown time scales are in units of unperturbed periods P of such trajectory, given by test particle the semi-major axis a value and the third Kepler law.

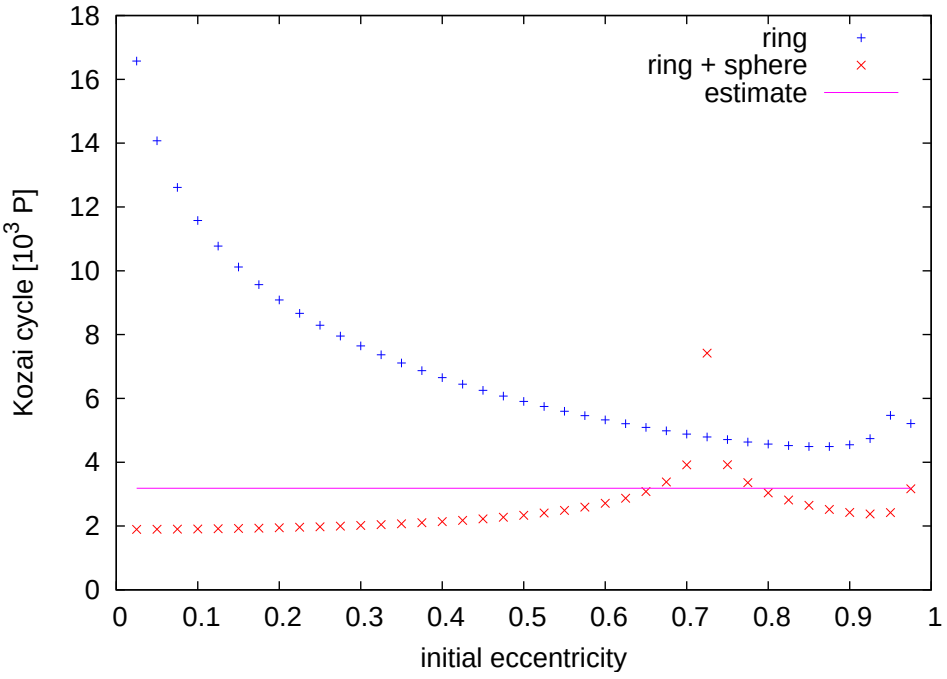

Figure 1.4: Kozai period as a function of initial eccentricity e_0 for trajectories with initial argument of periastre $\omega_0 = \pi/2$ influenced by composite perturbing potential from ring with $a_{\mathrm{RING}} = 10\ a$, $M_{\mathrm{RING}} = 5 \times 10^{-2} M_\bullet$ and from sphere with mass $M_{\mathrm{SPHE}} = 10^{-3} M_\bullet$ evaluated at $r_0 = 2\ a$ with the power-law index $\alpha = 1.4$. The test particle was the S2 star with $a = 13578.588 R_{\mathrm{g}}$ and the chosen value of Kozai constant was $c = 0.2$.

Bibliography

[1] Genzel R. et al. The stellar cusp around the supermassive black hole in the galactic center. *ApJ*, 594:812, 2003.

[2] Ivanov P. B. et al. The tidal disruption rate in dense galactic cusps containing a supermassive binary black hole. *MNRAS*, 358:1361, 2005.

[3] Mouawad N. et al. Stellar orbits at the center of the milky way. *Astron. Nachr.*, 324:315, 2003.

[4] Mouawad N. et al. Weighing the cusp at the galactic centre. *Astron. Nachr.*, 326:83, 2005.

[5] Binney J. and Merrifield M. *Galactic Astronomy*. Princeton University Press, 1998.

[6] Binney J. and Tremaine S. *Galactic Dynamics*. Princeton University Press, 1987.

[7] Spitzer L. *Dynamical Evolution of Globular Clusters*. Princeton University Press, 1987.

[8] Genzel R. and Townes C.H. Physical conditions, dynamics and mass distribution in the center of the galaxy. *Ann. Rev. AA*, 25:377, 1987.

[9] Press W.H., Teukolsky S.A., Vetterling W.T., and Flannery B.P. *Numerical Recipes, the Art of Scientific computing*. Cambridge University Press, 1992.

[10] Kozai Y. Secular perturbations of asteroids with high inclination and eccentricity. *AJ*, 67:591, 1962.